

Modified uvsY by N-Terminal Hexahistidine Tag Addition Enhances Efficiency of Recombinase Polymerase Amplification to Detect SARS-CoV-2 DNA.

Kevin Maafu Juma

Kyoto University Graduate School of Agriculture Faculty of Agriculture: Kyoto Daigaku Nogaku Kenkyuka Nogakubu

Teisuke Takita

Kyoto University Graduate School of Agriculture Faculty of Agriculture: Kyoto Daigaku Nogaku Kenkyuka Nogakubu

Masaya Yamagata

Kyoto University Graduate School of Agriculture Faculty of Agriculture: Kyoto Daigaku Nogaku Kenkyuka Nogakubu

Mika Ishitani

Kyoto University Graduate School of Agriculture Faculty of Agriculture: Kyoto Daigaku Nogaku Kenkyuka Nogakubu

Kaichi Hayashi

Kyoto University Graduate School of Agriculture Faculty of Agriculture: Kyoto Daigaku Nogaku Kenkyuka Nogakubu

Kenji Kojima

Himeji Dokkyo University: Himeji Dokkyo Daigaku

Koichiro Suzuki

The Research Foundation of Microbial Disease of Osaka University

Yuri Ando

Kansei Gakuin Daigaku

Shinsuke Fujiwara

Kansei Gakuin Daigaku

Yukiko Nakura

Osaka Women's and Children's Hospital: Osaka Boshi Iryo Center

Itaru Yanagihara

Osaka Women's and Children's Hospital: Osaka Boshi Iryo Center

Kiyoshi Yasukawa (✉ yasukawa.kiyoshi.7v@kyoto-u.ac.jp)

Kyoto University Graduate School of Agriculture Faculty of Agriculture: Kyoto Daigaku Nogaku Kenkyuka Nogakubu <https://orcid.org/0000-0001-7748-6043>

Research Article

Keywords: isothermal DNA amplification, hexahistidine tag, recombinase polymerase amplification (RPA), uvsY.

Posted Date: November 8th, 2021

DOI: <https://doi.org/10.21203/rs.3.rs-975844/v1>

License:   This work is licensed under a Creative Commons Attribution 4.0 International License.

[Read Full License](#)

Version of Record: A version of this preprint was published at Molecular Biology Reports on January 31st, 2022. See the published version at <https://doi.org/10.1007/s11033-021-07098-y>.

Abstract

Background

Recombinase (*UvsY* and *UvsX*) from bacteriophage T4 is a key enzyme for recombinase polymerase amplification (RPA) that amplifies a target DNA sequence at a constant temperature with a single-stranded DNA-binding protein and a strand-displacing polymerase. The present study was conducted to examine the effects of the N- and C-terminal tags of *UvsY* on its function in RPA to detect SARS-CoV-2 DNA.

Methods

Untagged *UvsY* (*UvsY*- Δ his), N-terminal tagged *UvsY* (*UvsY*-Nhis), C-terminal tagged *UvsY* (*UvsY*-Chis), and N- and C-terminal tagged *UvsY* (*UvsY*-NChis) were expressed in *Escherichia coli* and purified. RPA reaction was carried out with the *in vitro* synthesized standard DNA at 41°C. The amplified products were separated on agarose gels.

Results

The minimal initial copy numbers of standard DNA from which the amplified products were observed were 6×10^5 , 60, 600, and 600 copies for the RPA with *UvsY*- Δ his, *UvsY*-Nhis, *UvsY*-Chis, and *UvsY*-NChis, respectively. The minimal reaction time at which the amplified products were observed were 20, 20, 30, and 20 min for the RPA with *UvsY*- Δ his, *UvsY*-Nhis, *UvsY*-Chis, and *UvsY*-NChis, respectively. The RPA with *UvsY*-Nhis exhibited clearer bands than that with either of other three *UvsY*s.

Conclusion

The reaction efficiency of RPA with *UvsY*-Nhis was the highest, suggesting that *UvsY*-Nhis is suitable for use in RPA.

Introduction

Recombinase polymerase amplification (RPA) amplifies a target DNA sequence at a constant temperature around 37–42°C [1–3]. In RPA, recombinase (Rec) binds to the primers using its ATP hydrolysis activity. The primers of the resulting complex bind to the homologous sequence of the DNA template. Single-stranded DNA-binding protein (SSB) binds to the unwound strand. Strand-displacing DNA polymerase (Pol) extends the primer while SSB binds to the displaced strand. In this way, a new DNA strand is synthesized. Unlike PCR that requires thermal cycling, RPA eliminates the use of specialized equipment such as a thermal cycler. In view of this, most papers on RPA so far published have highlighted the importance of RPA in point-of-care use. Indeed, main RPA targets are pathogenic

organisms. Furthermore, RPA is applicable to detect RNA including SARS-CoV-2 RNA by combining with reverse transcriptase [4–6].

Since the first report of RPA [1], T4 phage *UvsX* and *UvsY* have been used as Rec, T4 phage gp32 as SSB, and *Bacillus subtilis* (*Bst*) DNA polymerase as Pol. *UvsX* binds to the primers, while *UvsY*, originally identified as the T4 recombination mediator protein acts as the loading factor to assist *UvsX* to bind to the primers [7]. In earlier studies, we prepared recombinant *UvsX*, *UvsY*, and gp32 using an *Escherichia coli* expression system [8]. We also examined the effects of each component of the reaction solution on the RPA reaction efficiency and optimized the reaction conditions using a statistical method [5]. In those studies, *UvsX*, *UvsY*, and gp32 were expressed as N- and C-terminal hexahistidine-tagged (His-tagged) proteins with a thrombin recognition site. Purification was carried out from the cells by ammonium sulfate fractionation and Ni²⁺ affinity column chromatography. When treated with thrombin to cleave the His-tag, *UvsY* became insoluble while *UvsX* and gp32 remained soluble [8]. Therefore, we used untagged *UvsX* and gp32 and N- and C-terminal tagged *UvsY* to optimize reaction conditions [5]. However, it is possible that the uncleaved tag has a negative effect on the RPA reaction. In this study, we examined the effects of N- and C-terminal His-tags of *UvsY* on its function in RPA using SARS-CoV-2 DNA as a model target.

Materials And Methods

Materials

UvsX and gp32 were expressed in *Escherichia coli*, as N- and C-terminal His-tagged proteins with a thrombin recognition site and purified from the cells, and the tags were removed by thrombin treatment as described previously [8]. The concentrations of *UvsX* and gp32 were determined using the molar absorption coefficient at 280 nm of 33,015 and 41,160 M⁻¹ cm⁻¹, respectively. *Bst* DNA polymerase (large fragment) was purchased from New England BioLabs (Ipswich, MA). Creatine kinase was purchased from Roche (Mannheim, Germany).

Construction of plasmids

Construction of pET-*UvsY*-NChis, previously termed pET-*UvsY*2, was described previously [8]. For the construction of pET-*UvsY*-NChis-2 (Supplementary Figure 1), the DNA fragment was amplified from pET-*UvsY*-NChis using primers *UvsY*_N-thrombin-del_F (GGCAGCCATATGATGAGATTAGAAGATC) and *UvsY*_N-thrombin-del_R (GTGATGATGATGATGATGGCTGCTG) with 35 cycles at 98°C for 10 s and 68°C for 5 min. The amplified fragment was phosphorylated at its 5' terminus with T7 polynucleotide kinase and self-ligated. For the construction of pET-*UvsY*-Nhis, the DNA fragment was amplified from pET-*UvsY*-NChis-2 using primers *UvsY*_N-His-only_F (TGAGATCCGGCTGCTAACAAAGC) and *UvsY*_N-His-only_R (TTTTCCAGCCTCAAATGCTCG) with 35 cycles at 98°C for 10 s and 68°C for 5 min. The amplified fragment was phosphorylated and self-ligated. For the construction of pET-*UvsY*-Chis, the 168-bp DNA fragment corresponding to 161–328 of pET-22b(+) (Merck Millipore, Burlington, MA) was inserted into the

*Xba*I and *Xho*I sites of pET-28a(+) (Merck Millipore). To the *Nde*I and *Xho*I sites of the resulting plasmid, the *Nde*I- and *Xho*I-digested 411-bp *UvsY* DNA fragment of pET-*UvsY*-1 (Supplementary Figure 1), corresponding to DNA sequence 114,929–115,339 deposited in GenBank (KJ477686.1), was inserted. For the construction of pET-*UvsY*- Δ his, the DNA fragment was amplified from pET-*UvsY*-Chis using primers *UvsY*_N-His-only_F and *UvsY*_N-His-only_R with 35 cycles at 98°C for 10 s and 68°C for 5 min. The amplified fragment was phosphorylated and self-ligated.

Expression of *UvsY*

Each of the four plasmids were transfected into *E. coli* BL21(DE3) [F^- , *ompT*, *hsdS_B*(r_B^- m_B^-) *gal dcm* (DE3)]. The overnight culture of the transformants (30 mL) was added to 300 mL of L broth containing 50 μ g/mL kanamycin and incubated with shaking at 37°C. When OD_{660} reached 0.6–0.8, the culture (300 mL) was added to 2,000 mL of L broth containing 50 μ g/mL kanamycin, and 2.0 mL of 0.5 M IPTG was added. Growth was continued at 30°C for 4 h. The cells were harvested by the centrifugation of the culture at 3,000 \times g for 10 min and suspended with 50 mL of 50 mM phosphate buffer (pH 7.2), 1 M NaCl, 2 mM phenylmethylsulfonyl fluoride (PMSF), and disrupted by sonication. After centrifugation at 20,000 \times g for 20 min, the supernatant was collected as the soluble fraction of the cells.

Purification of *UvsY*- Δ his

Solid $(\text{NH}_4)_2\text{SO}_4$ was added to the soluble fraction of the cells to a final concentration of 30% saturation. Following the centrifugation at 20,000 \times g for 20 min, the supernatant was collected and adjusted to a final concentration of 80% saturation. Following the centrifugation, the pellet was collected and dissolved in 100 mL of buffer A (50 mM Tris-HCl (pH 8.0), 1 mM dithiothreitol (DTT)) and applied to the column packed with Toyopearl DEAE-650M (Tosoh, Tokyo, Japan) equilibrated with buffer A. After washing with buffer A, the bound *UvsY*- Δ his was eluted with each 20 mL of buffer A containing 100, 200, and 300 mM NaCl. Each fraction (5 mL) was assessed for the presence of *UvsY*- Δ his by SDS-PAGE. The active fractions were collected, concentrated to 1 mL in 10 mM Tris-HCl by Amicon Ultra-15 MWCO 10 k (Merck Millipore, Burlington, MA), and stored in 10 mM Tris-HCl, 20% v/v glycerol at -30°C . The *UvsY*- Δ his concentration was determined by the method of Bradford using Protein Assay CBB Solution (Nacalai Tesque, Kyoto, Japan) with bovine serum albumin (Nacalai Tesque) as standard.

Purification of *UvsY*-Nhis, *UvsY*-Chis, and *UvsY*-NChis

Solid $(\text{NH}_4)_2\text{SO}_4$ was added to the soluble fraction of the cells to a final concentration of 40% saturation. In *UvsY*-NChis, following the centrifugation, the pellet was dissolved in 50 mL of buffer B (50 mM phosphate buffer (pH 7.2), 500 mM NaCl). In *UvsY*-Nhis and *UvsY*-Chis, following the centrifugation, the supernatant was collected and adjusted to a final concentration of 60% and 80% saturation, respectively. Following the centrifugation, the pellet was dissolved in 50 mL of buffer B. The solution was applied to the column packed with a Ni^{2+} -sepharose (Profinity IMAC resin 5 mL, BioRad, Hercules, CA) equilibrated with buffer B. After washing with 100 mL buffer B containing 100 mM imidazole, the bound enzyme was eluted with 50 mL of buffer B containing 600 mM imidazole. The active fractions were collected and

concentrated as described above. The uvsY concentration was determined by the method of Bradford as described above.

Solubility test

UvsY (0.2 µg/mL in 50 mM Tris-HCl buffer (pH 8.6)) was incubated at 42°C for specified time (10–60 min) followed by the centrifugation at 15,000 × *g* for 10 min. The absorbance at 280 nm (A_{280}) of the supernatant was measured with a Jasco spectrophotometer model V-550 (Japan Spectroscopic Company, Tokyo, Japan).

RPA reaction

The RPA detection system for SARS-CoV-2 DNA was used (Supplementary Figure 2) [5]. Unless otherwise indicated, the reaction condition was 400 ng/µL uvsX, 40 ng/µL uvsY, 400 ng/µL gp32, 0.4 units/µL *Bst* DNA polymerase, 120 ng/µL creatine kinase, 2 mM DTT, 6% PEG35000, 3.5 mM ATP, 650 mM dNTPs, 50 mM Tris-HCl buffer (pH 8.6), 40 mM CH₃COOK, 20 mM phosphocreatine, 8 mM Mg(OCOCH₃)₂, 1 µM 2F-15 primer, 1 µM 2R-11 primer at 41°C for 30 min. The reaction was performed in a 0.2 ml PCR tube in PCR Thermal Cycler Dice (Takarabio, Kusatsu, Japan). The amplified products were separated on 2.0% (w/v) agarose gels and stained with ethidium bromide (1 µg/ml).

Results And Discussion

Design and preparation of recombinant uvsY with or without His-tag

The His-tag is known to facilitate the purification of recombinant proteins. However, it sometimes decreases the solubility and activity of proteins [9]. We previously expressed recombinant uvsX, uvsY, and gp32 as N- and C-terminal His-tagged proteins with a thrombin recognition site. In uvsX and gp32, the tags were removed by thrombin treatment. Meanwhile, thrombin treatment of the N- and C-terminal His-tagged uvsY (UvsY-NChis) resulted in precipitation [8]. Fortunately, untreated uvsY-NChis was functional in the RPA reaction [8], indicating that the His-tag of uvsY does not abolish its function in RPA. However, it is possible that the uncleaved His-tag decreases the function of uvsY. To address this issue, we designed three new forms of uvsY, i.e., untagged uvsY (UvsY-Δhis), N-terminal His-tagged uvsY (UvsY-Nhis), and C-terminal His-tagged uvsY (UvsY-Chis). Figure 1 shows the *E. coli* expression plasmids for these three uvsYs and uvsY-NChis.

These four genes were expressed in *E. coli* BL21(DE3) cells. Purification was based on the procedure we previously described [8], but with several modifications. First, polyethyleneimine treatment of the soluble fraction of the cells, which was originally included to remove nucleic acids, was excluded. This prevented the viscosity of the solution from becoming so high that the flow rate of the successive Ni²⁺ affinity column chromatography was reduced. Second, ammonium sulfate fractionation was used instead. The ammonium sulfate concentrations at which uvsY-Δhis, uvsY-Nhis, uvsY-Chis, and uvsY-NChis

precipitated were 80%, 60%, 80%, and 40% saturation, respectively, indicating that the uvsY-NChis was the least soluble. From a 2 L culture, 25, 11, 11, and 9 mg of uvsY- Δ his, uvsY-Nhis, uvsY-Chis, and uvsY-NChis were obtained.

Figure 2 shows the results of the SDS-PAGE analysis of the active fractions at each purification stage and the purified enzyme preparations. The purified uvsY- Δ his, uvsY-Nhis, uvsY-Chis, and uvsY-NChis preparations yielded single bands with molecular masses of 16, 17, 17, and 22 kDa, respectively. The molecular masses of these uvsYs calculated from the amino acid sequences were 15,952, 17,419, 17,159, and 19,847 Da, respectively (Fig. 1), indicating that the two molecular masses were considerably different for uvsY-NChis, but were almost similar for uvsY- Δ his, uvsY-Nhis, and uvsY-Chis. These results suggested that when both the N- and C-terminal His-tags were present, the structure of uvsY was considerably altered.

Comparison of the solubility of uvsY with or without His-tag

The remaining soluble protein concentration was determined after thermal treatment at 42°C. The natural logarithm of the soluble fraction was plotted against the incubation time (Fig. 3). The soluble fraction of uvsY- Δ his were stable. The soluble fraction of uvsY-Nhis decreased to 15% at 60 min. The soluble fractions of uvsY-Chis and uvsY-NChis decreased more rapidly than did uvsY-Nhis, and decreased to less than 5% at 60 min. These results indicated that the solubility was in the order of uvsY- Δ his > uvsY-Nhis > uvsY-Chis \approx uvsY-NChis, suggesting that the presence of His-tag, especially C-terminal His-tag, reduced the solubility of uvsY.

Comparison of the optimal concentration of uvsY with or without His-tag in RPA

The effect of each uvsY concentration on the RPA reaction efficiency was examined. For this purpose, the RPA detection system for SARS-CoV-2 (Supplementary Figure 2), which we established previously [5], was used. Figure 4 shows the analysis of the products in the RPA reaction with each uvsY using agarose gel electrophoresis. The uvsY concentrations at which amplified DNA band was observed were 10–20 ng/ μ L for uvsY- Δ his, 10–40 ng/ μ L for uvsY-Nhis, 10–100 ng/ μ L for uvsY-Chis, and 40–100 ng/ μ L for uvsY-NChis. Non-specific bands were observed at 10–100 ng/ μ L uvsY- Δ his.

Our previous results indicated that uvsY concentrations that are too low or excessive are detrimental for the reaction [5]. These findings were also evident for uvsX, gp32, and ATP [5]. Thus, our results suggested that the specific activity of uvsY-Nhis was higher than those of the other three uvsY. We set 20, 20, 80, and 60 ng/ μ L as the optimal concentrations of uvsY- Δ his, uvsY-Nhis, uvsY-Chis, and uvsY-NChis, respectively, and conducted the subsequent experiments.

It was first reported that by gel-shift assay, uvsX, uvsY, and gp32 form a ternary complex with a single-stranded DNA (ssDNA) [10]. The presence of the ternary complex was also observed using surface

plasmon resonance and isothermal titration calorimetry [11]. However, binding of uvsY to ssDNA lessens the subsequent binding of the ssDNA to gp32 [11]. Thus, uvsY and gp32 bind to ssDNA competitively. In the RPA process, this competition should be adjusted to achieve a high reaction efficiency by optimizing the concentrations of uvsX, uvsY, gp32, and ATP. If the binding of uvsY to DNA primer is not strong enough, the binding of uvsX to DNA primer will also not be strong enough. Thus, the DNA primer cannot invade double-stranded DNA, preventing it from binding to the target sequence. In contrast, if the binding of uvsY to DNA primer is too strong, the binding of uvsX to the DNA primer will be also too strong, and uvsX will remain occupied even after the elongation starts. This will prevent another nucleoprotein from binding to the target sequence and initiating the elongation.

Comparison of sensitivity and speed of RPA reaction using uvsY with or without His-tag

For comparison of sensitivity, RPA reaction was carried out using each uvsY with $60-6 \times 10^7$ copies of standard DNA at 41°C for 30 min. In the analysis of the products in the subsequent electrophoresis, the minimal initial copy numbers of standard DNA from which the amplified products were observed were 6×10^5 , 60, 600, and 600 copies for the RPA with uvsY- Δ his, uvsY-Nhis, uvsY-Chis, and uvsY-NChis, respectively (Fig. 5). Several non-specific bands were observed at $0-6 \times 10^3$ copies for the RPA with uvsY- Δ his (lanes 1-4 in Fig. 5A),

For comparison of speed, RPA reaction was carried out using each uvsY with 6,000 copies of standard DNA at 41°C for 10-60 min. The minimal reaction time at which the amplified products were observed were 20, 20, 30, and 20 min for the RPA with uvsY- Δ his, uvsY-Nhis, uvsY-Chis, and uvsY-NChis, respectively (Fig. 6). More importantly, the RPA with uvsY-Nhis exhibited clearer bands than that with either of other three uvsYs. These results indicated that the reaction efficiency of RPA with uvsY-Nhis was higher than that with either of the other three.

The first crystallographic analysis of uvsY reported that uvsY exists as a hexamer [12]. A more recent crystallographic analysis revealed that it exists as a heptamer and that one uvsY molecule consists of four α -helices (H1-H4: H1, E5-Y14; H2, L21-S65; H3, K80-S88; and H4, K91-E134) [11]. When viewed from the top of the heptamer, H4 is located inside, whereas H1, H2, and H3 are located outside. In one heptamer, seven N-terminal residues are located apart from each other and seven C-terminal residues are located close together. In this study, the presence of a C-terminal His-tag of uvsY reduced its function in RPA (Figs. 4-6). It was previously described that cleavage of the His-tag by thrombin rendered uvsY-NChis insoluble [8]. These results might be explained as follows. In the heptameric assembly, C-terminal peptides containing His-tag and thrombin recognition sequence in close proximity to each other alter the uvsY structure unfavorably, leading to decreased activity and precipitation by thrombin treatment. The results of solubility test (Fig. 3) supports this hypothesis. uvsY- Δ his exhibited higher solubility than other three uvsYs (Fig. 3). As for its low activity (Figs. 4-6), we presume that the preparation contained some impurities, such as nucleic acid, that inhibited the RPA reaction. Such impurities can be removed using Ni^{2+} affinity chromatography.

In conclusion, the reaction efficiency of RPA with N-terminal tagged *uvrY* was higher than that with untagged *uvrY*, C-terminal tagged *uvrY*, or N- and C-terminal tagged *uvrY*. Our results enhance the flexibility in fabricating RPA reagents for point-of-care use.

Abbreviations

RPA, recombinase polymerase amplification; SSB, single-stranded DNA-binding protein.

Declarations

Acknowledgments We acknowledge Mr. Kenji Ito for his technical assistance.

Author contributions KMJ, TT, and KY designed the research; KMJ, TT, MY, MI, KH, KK, YA and YN performed the research; KMJ, TT, KK, KS, SF, YN, IY, and KY analyzed data; KMJ and KY wrote the manuscript.

Data availability All data are available in case of need.

Compliance with Ethical Standards

Consent for publication All authors agree for publication

Funding This work was supported in part by Grants-in-Aid for Scientific Research (no. 18KK0285 for T.T., K.K., and K.Y.) from Japan Society for the Promotion of Science, Emerging/re-emerging infectious disease project of Japan (grant no. 20he0622020h0001 for S.F., I.Y., K.Y. and grant no. 20fk0108143h001 for S.F., I.Y., K.Y.) from Japan Agency for Medical Research and Development, and A-Step (no. JPMJTR20UU for K.Y.) from Japan Science and Technology Agency.

Conflict of interest Authors declare that they have no conflict of interests.

Research involved in human or animal rights No experiment was conducted on animals in this study.

References

1. Piepenburg O, Williams CH, Stemple DL, Armes NA (2006) DNA detection using recombination proteins. *PLoS Biol.* 4:e204
2. Lobato IM, O'Sullivan CK (2018) Recombinase polymerase amplification: Basics, applications and recent advances. *Trends Analyt Chem* 98:19–35
3. Li J, Macdonald J, von Stetten F (2019) Review: a comprehensive summary of a decade development of the recombinase polymerase amplification. *Analyst* 144:31–67
4. Wu T, Ge Y, Zhao K, Zhu X, Chen Y, Wu B, Zhu F, Zhu B, Cui L (2020) A reverse-transcription recombinase-aided amplification assay for the rapid detection of N gene of severe acute respiratory syndrome coronavirus 2 (SARS-CoV-2). *Virology* 549:1–4

5. Juma KM, Takita T, Ito K, Yamagata M, Akagi S, Arikawa E, Kojima K, Biyani M, Fujiwara S, Nakura Y, Yanagihara I, Yasukawa K (2021) Optimization of reaction condition of recombinase polymerase amplification to detect SARS-CoV-2 DNA and RNA using a statistical method. *Biochem Biophys Res Commun* 56:195–200
6. Lau YL, Ismail IB, Mustapa NIB, Lai MY, Tuan Soh TS, Haji Hassan A, Peariasamy KM, Lee YL, Abdul Kahar MKB, Chong J, Goh PP (2021) Development of a reverse transcription recombinase polymerase amplification assay for rapid and direct visual detection of Severe Acute Respiratory Syndrome Coronavirus 2 (SARS-CoV-2). *PLoS One* 16:e0245164
7. Bleuit JS, Xu H, Ma Y, Wang T, Liu J, Morrical SW (2001) Mediator proteins orchestrate enzyme-ssDNA assembly during T4 recombination-dependent DNA replication and repair. *Proc Natl Acad Sci USA* 98:8298–8305
8. Kojima K, Juma KM, Akagi S, Hayashi T, Takita T, O'Sullivan CK, Fujiwara S, Nakura Y, Yanagihara I, Yasukawa K (2021) Solvent engineering studies on recombinase polymerase amplification. *J Biosci Bioeng* 131:219–224
9. Terpe K. (2003) Overview of tag protein fusions: from molecular and biochemical fundamentals to commercial systems. *Appl Microbiol Biotechnol* 60:523–533
10. Hashimoto K, Yonesaki T (1991) The characterization of a complex of three bacteriophage T4 recombination proteins, uvsX protein, uvsY protein, and gene 32 protein, on single-stranded DNA. *J Biol Chem* 266 (1991) 4883–4888
11. Gajewski S, Waddell MB, Vaithiyalingam S, Nourse A, Li Z, Woetzel N, Alexander N, Meiler J, White SW (2016) Structure and mechanism of the phage T4 recombination mediator protein UvsY. *Proc Natl Acad Sci USA* 113:3275–3280
12. Xu H, Beernink HTH, Rould MA, Morrical SW (2006) Crystallization and preliminary X-ray analysis of bacteriophage T4 UvsY recombination mediator protein. *Acta Crystallogr Sect F Struct Biol Cryst Commun* 62:1013–1015

Figures

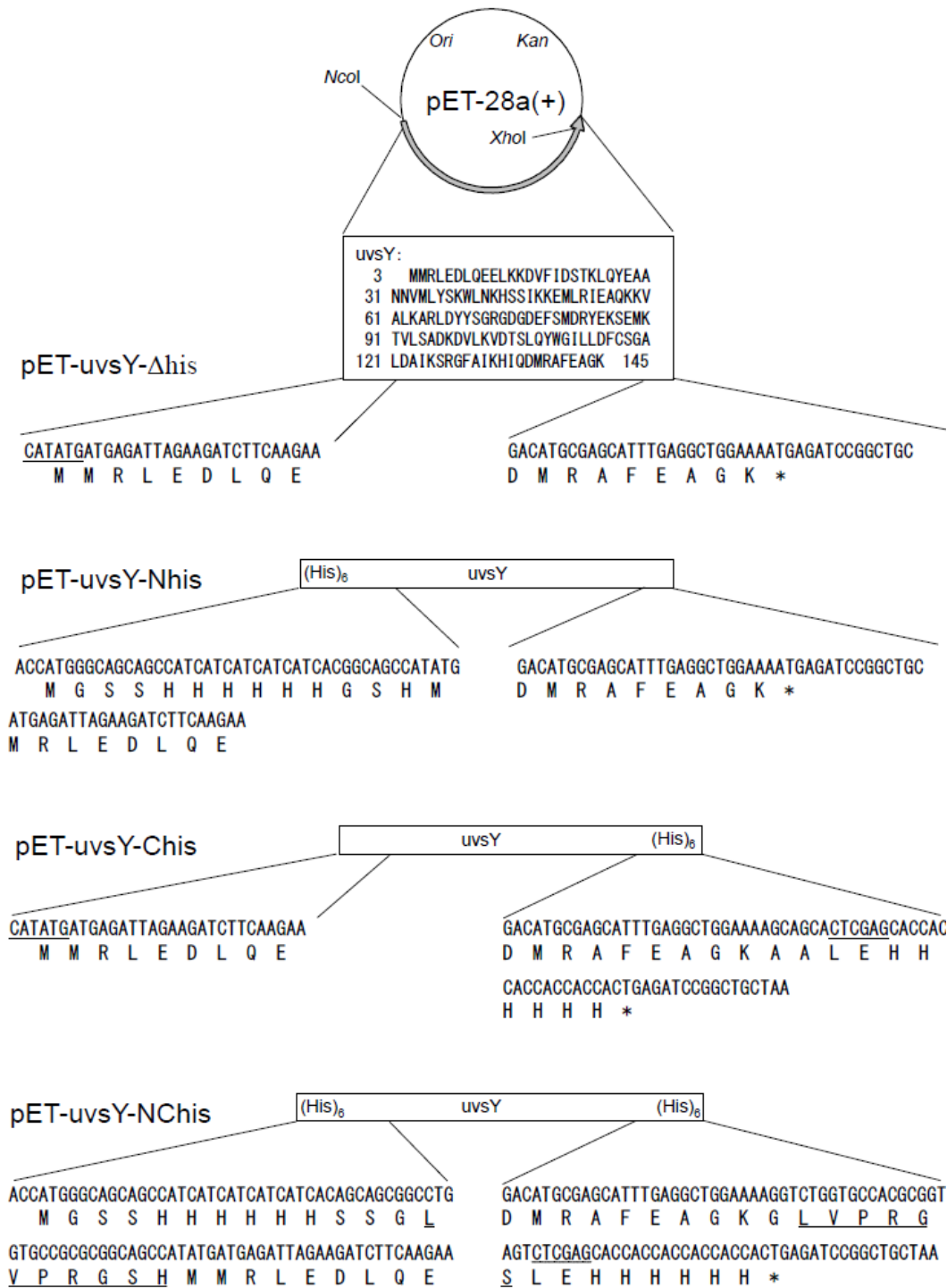


Figure 1

Expression plasmids. The asterisk indicates the termination codon. The thrombin recognition sequence and NdeI and XhoI sites are underlined.

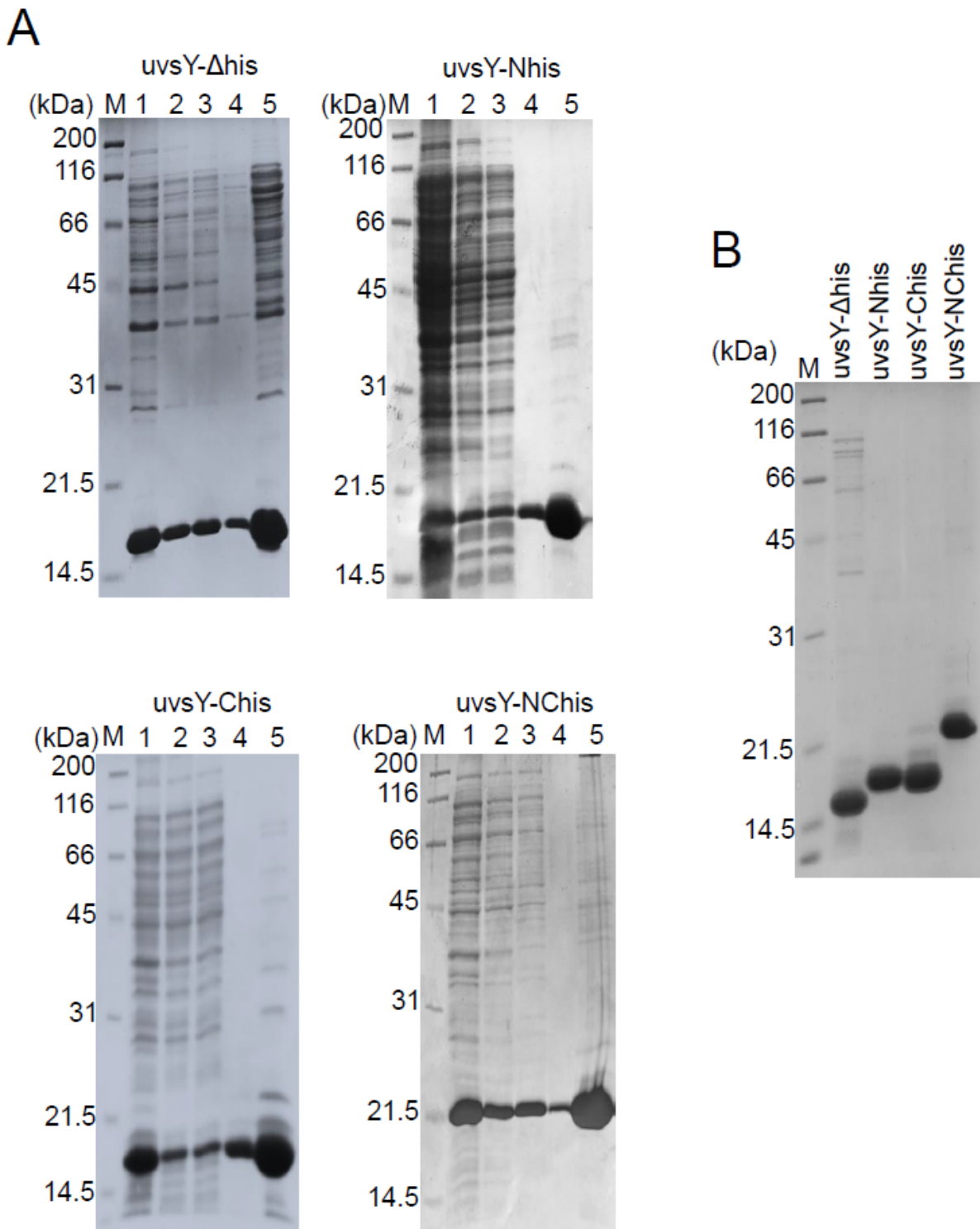


Figure 2

Purification of *uvsY*. SDS-PAGE was conducted under reducing conditions. Coomassie Brilliant Blue-stained 12.5% SDS-polyacrylamide gels are shown. (A) Marker proteins (lane M), total cell extracts (lane 1), soluble fractions of the total cell extracts (lane 2), the centrifuged pellets after fractionation by ammonium sulfate (lane 3), active fractions of anion-exchange chromatography for *uvsY- Δ his* and Ni²⁺ affinity chromatography for *uvsY-Nhis*, *uvsY-Chis*, and *uvsY-NChis* (lane 4), and purified preparations

after membrane concentration (lane 5). (B) Purified preparations. The arrow indicates the band corresponding to *uvrY*.

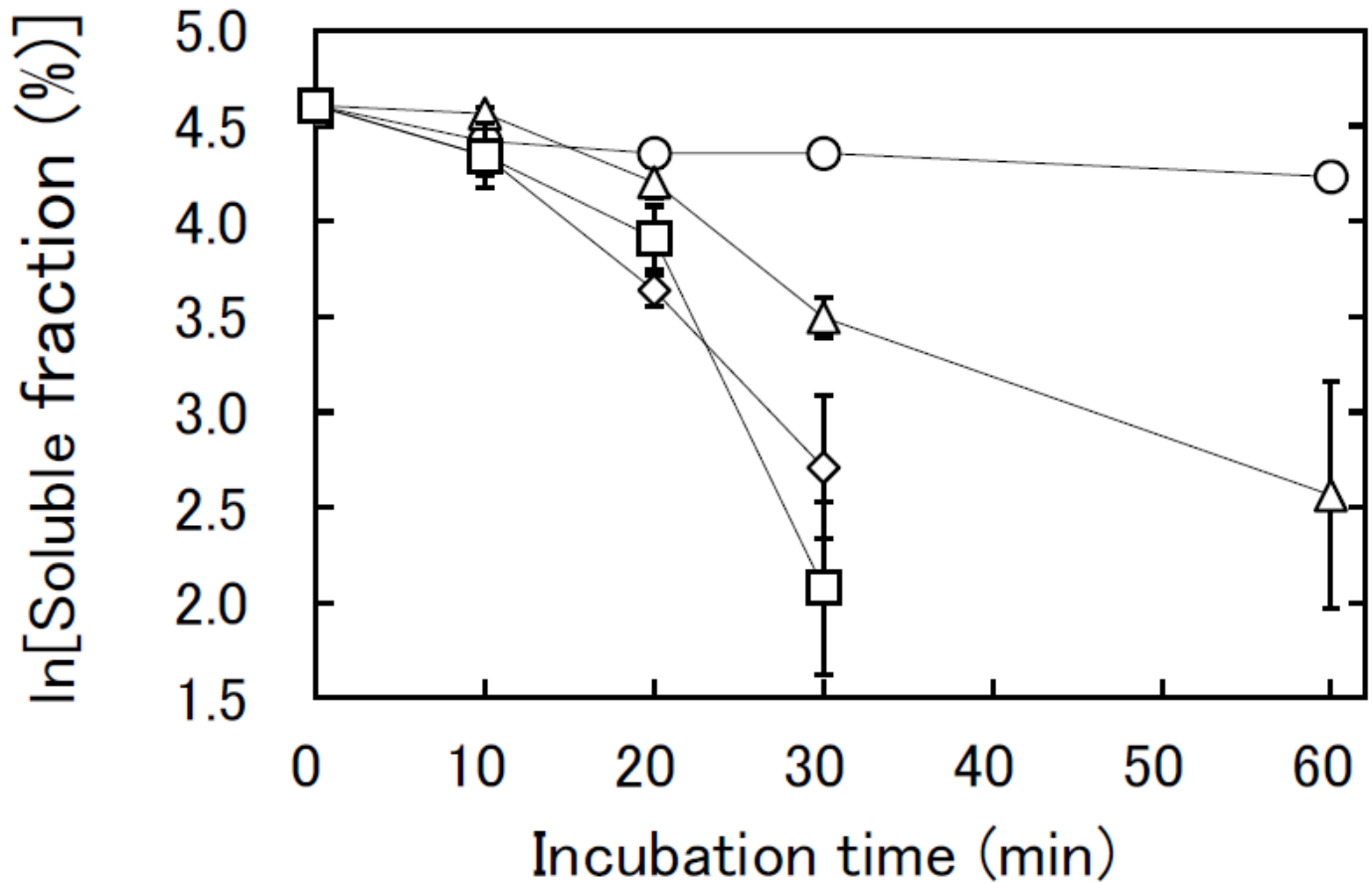


Figure 3

Effects of thermal incubation on the solubility of *uvrY*. *uvrY*- Δ his (open circle), *uvrY*-Nhis (open triangle), *uvrY*-Chis (open square), or *uvrY*-NChis (open diamond) each at 0.2 μ g/mL was incubated at 42°C for the indicated durations. Then, the soluble *uvrY* concentration was determined. The soluble fraction was defined as the ratio of the concentration of soluble *uvrY* with incubation for the indicated durations to that without incubation. Error bars indicate SD values. The average of triplicate determination is shown.

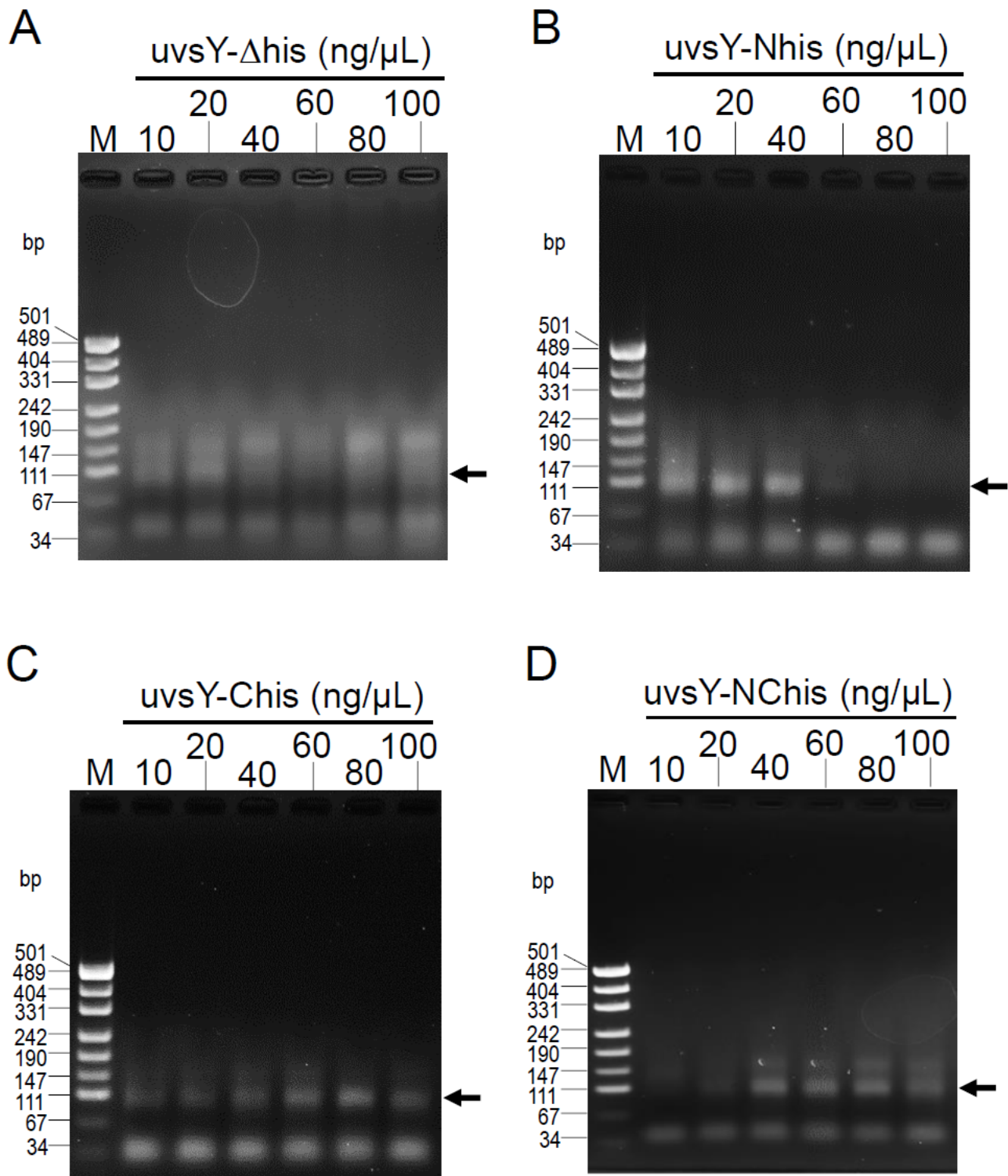


Figure 4

Effects of the concentrations of *uvyY* on the reaction efficiency of RPA. The reactions were carried out with 10, 20, 40, 60, 80, and 100 ng/ μ L *uvyY- Δ his* (A), *uvyY-Nhis* (B), *uvyY-Chis* (C), or *uvyY-NChis* (D) at 41°C for 30 min. Initial copies of standard DNA was 6,000. The arrow indicates the 99-bp target band.

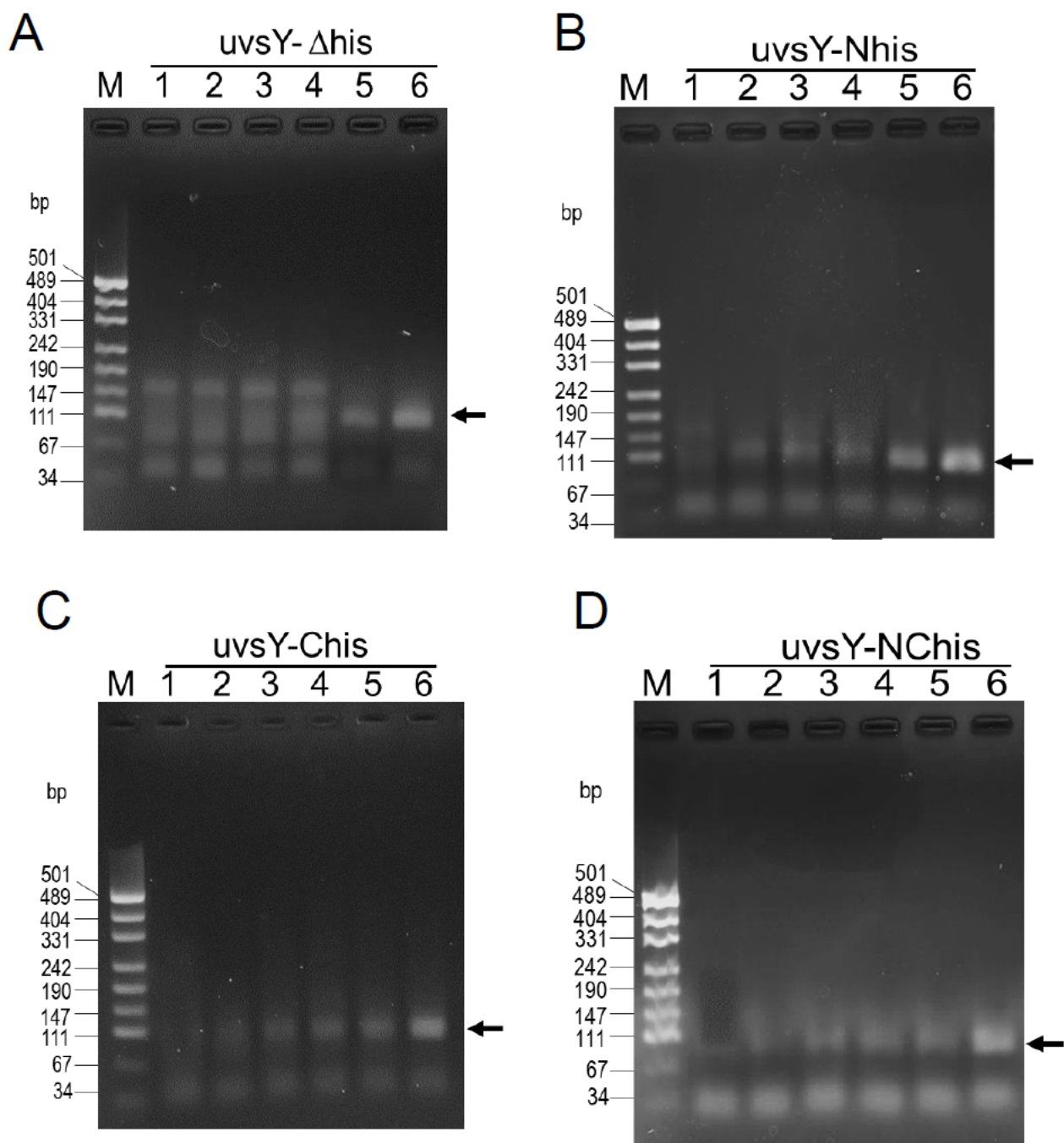


Figure 5

Effects of initial copies on the RPA reaction. The reactions were carried out with 20 ng/μL uvsY-Δhis (A), 20 ng/μL uvsY-Nhis (B), 80 ng/μL uvsY-Chis (C), or 60 ng/μL uvsY-NChis (D) at 41°C for 30 min. Initial copies of standard DNA: 0 (lane 1), 60 (lane 2), 600 (lane 3), 6×10^3 (lane 4), 6×10^5 (lane 5), and 6×10^7 (lane 6). The arrow indicates the 99-bp target band.

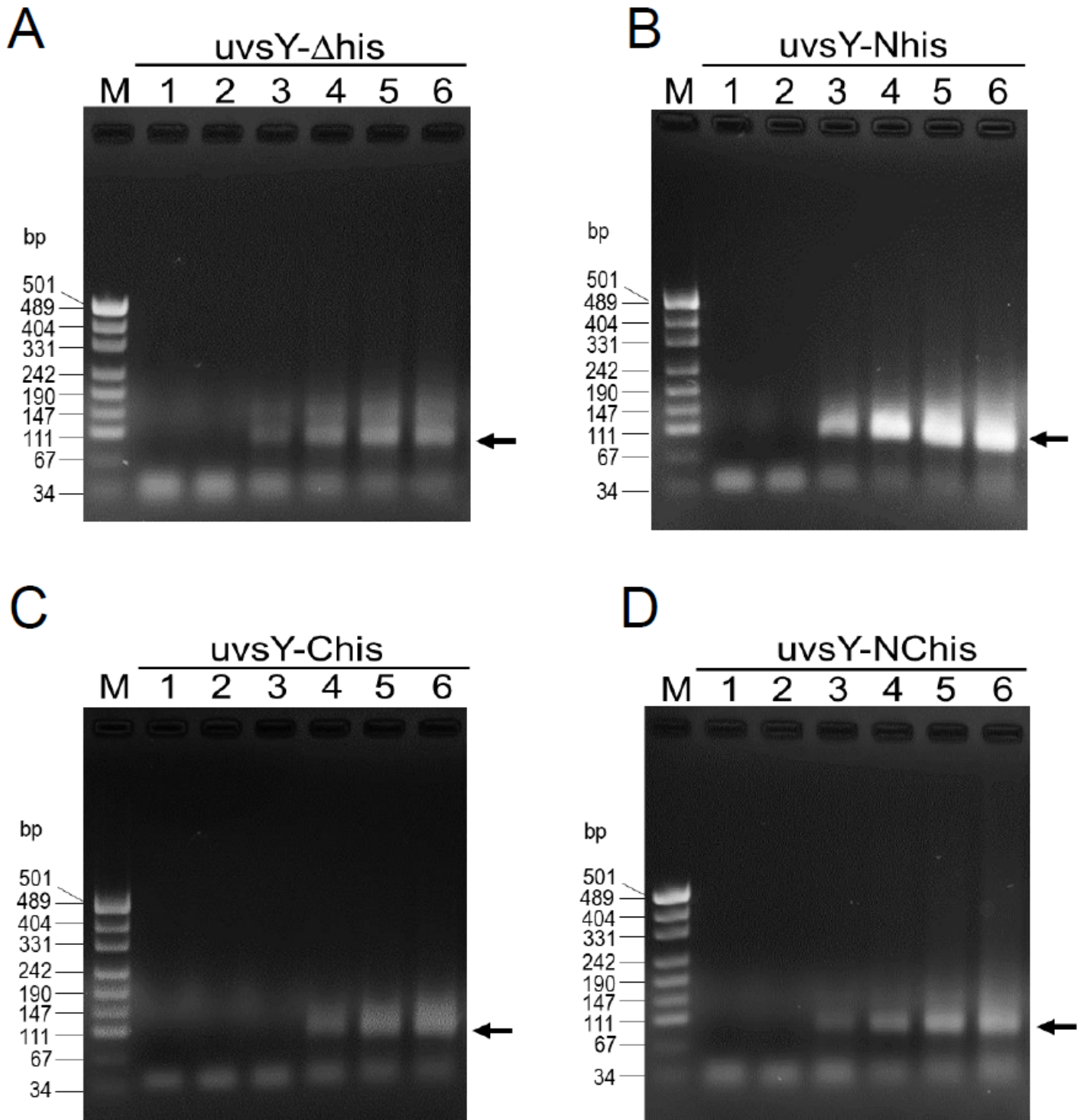


Figure 6

Effects of reaction time on the RPA reaction. The reactions were carried out with 400 ng/ μ L *uvsX*, 40 ng/ μ L *uvsY- Δ his* (A), *uvsY-Nhis* (B), *uvsY-Chis* (C), or *uvsY-NChis* (D) at 41°C for 0–60 min. Initial copies of standard DNA was 6,000. Reaction time (min): 0 (lane 1), 10 (lane 2), 20 (lane 3), 30 (lane 4), 45 (lane 5), and 60 (lane 6).

Supplementary Files

This is a list of supplementary files associated with this preprint. Click to download.

- [JumaSFig211015.pdf](#)